The Journal of Veterinary Medical Science

FULL PAPER

Anatomy

Fibrillar architecture at three different sites of the bovine superficial digital flexor tendon

Naoki TAKAHASHI[1)], Takuya HIROSE[1)], Jun A. MINAGUCHI[1], Hiromi UEDA[2)], Prasarn TANGKAWATTANA[1,3)]* and Kazushige TAKEHANA[1)]

[1)]Laboratory of Veterinary Microanatomy, School of Veterinary Medicine, Rakuno Gakuen University, Ebetsu, Hokkaido 069-8501, Japan

[2)]Laboratory of Veterinary Anatomy, School of Veterinary Medicine, Rakuno Gakuen University, Ebetsu, Hokkaido 069-8501, Japan

[3)]Department of Veterinary Anatomy, Faculty of Veterinary Medicine, Khon Kaen University, Khon Kaen, 40002, Thailand

J. Vet. Med. Sci.
80(3): 405–412, 2018
doi: 10.1292/jvms.17-0562

Received: 17 October 2017
Accepted: 28 December 2017
Published online in J-STAGE: 12 January 2018

ABSTRACT. Superficial digital flexor tendon (SDFT) of the bovine hindlimb originates from the caudolateral aspect of the distal femur and finally inserts onto the plantar aspect of the middle phalanges. In the present study, morphology and morphometry of the bovine SDFT at the muscle-tendon junction (MTJ), middle metatarsus (mM) and tendon-bone interface (TBI) were investigated. Cross-sectional morphology at the three regions of SDFT were oval, semioval and ring-formed, respectively. Significant difference in cross-sectional area was found only between MTJ-mM and mM-TBI ($P<0.05$). Functional compression and friction from the adjacent structures could be the most potential interactions affecting such appearances. Morphometric data of tenocyte number, water content, and glycosaminoglycan (GAG) length and angle were found increasing in the proximodistal direction, except the fibril diameter and collagen fibril index (CFI). Statistical analyzes could reveal significant differences in average number of tenocytes ($P<0.0001$), CFI (between MTJ-mM and MTJ-TBI, $P<0.05$), water content (between MTJ-TBI, $P<0.05$), length of GAG chains (between MTJ-TBI, $P<0.05$), and angle of GAG chains ($P<0.0001$), respectively. The fibrillar characteristics at the three different areas, including fibril diameter distribution and interfibrillar distance, existed in conforming to the tensional axes in situ. In addition, length and angle of GAG chains were relevant to moving directions of the collagen fibrils.

KEY WORDS: bovine, collagen fibril, glycosaminoglycans, morphometry, superficial digital flexor tendon

Tendon disorders in bovine species, e.g. laxity, contraction, inflammation, laceration, rupture, and tenosynovitis, could be the results of metabolic diseases (especially downer cow syndrome), infectious diseases, and direct trauma or injury to the nerves and locomotor apparatus, including bones, muscles, and tendons. The animals suffering from such disorders may be culled due to inability to stand, persistent lameness, loss of productivity, etc., which could deliver immense economic impacts to the livestock industry. Tendon disorders were indicated to involve 21% of limb lesions [18]. In bovine hindlimb, superficial digital flexor tendon (SDFT) initally runs between both heads of the gastrocnemius muscle and finally emerges with its tendon to form the major part of the Achilles tendon. After expanding to cap on the calcaneal tuberosity, SDFT courses along the plantar surface of the metatarsus and separates into medial and lateral parts at the distal end of the metatarsus. Each part then finally inserts on the plantar aspect of the middle phalanx of the same side. It has been known that thickness and density of collagenous population in each area of the same tendon is inconsistent [27]. Cross-sections of tendons upon approaching the bone interface may vary as flat, cylindrical, fan, or ribbon in shapes [11]. Such differences in transecting characteristics would reflect the uneven response to tension exerting on each part of the tendon [12]. Pertaining to these localities, different morphology and morphometry of the tendon and its fibrillar components between the proximal, middle and distal portions should reflect functions and vulnerability to injury of the tendon. This matter is crucial since injury of SDFT was reported to be about 30% of the causes of bovine locomotory disorders, e.g., tendon laceration and traumatic tendinitis at upper and middle part of SDFT and flexor tendon laxity, flexural deformities and fetlock contracture at its insertion [2]. Treatment to restore fibrillary integrity and regain normal function of the

*Correspondence to: Tangkawattana, P.: prasarn@kku.ac.th

injured tendon usually takes long time. Thus, a better understanding in microarchitecture of its fibrillar components will be beneficial for further therapeutic applications.

Tendon is considered as a special connective tissue with unique orientation of collagen fibrils; thus, allowing it to be histologically classified as a collagenous type of dense regular connective tissue. Approximately, 60% of tendon components are fluid that intersperses in the cellular and extracellular matrix (ECM) compartments. The ECM contains both fibrous and non-fibrous components. Collagen is the main fibrous population while proteoglycans (PG) and glycosaminoglycans (GAG) are abundantly in the non-fibrous compartment [11]. Collagen fibril is considered to be the primary unit being responsible for resisting tension in the tendon [5]. Behavior of collagen fiber to stress is highly dependent on length and width of collagen fibrils and density of cross-linking molecules [24]. Thus far, distribution of collagen fibril diameter at various sites on tendon of human, horse, and rat (either with or without exercise) was identified to be different [5, 12, 14, 15, 17, 26]. However, detailed morphological characterization of bovine SDFT, including cross-sectional shape and diameter, number of tendon cell, collagen fibril diameter, collagen fibril index, GAG chain, and moisture, seems lacking. The present study; therefore, analyzed these crucial basic structures of the SDFT in hindlimb of mature normal cows.

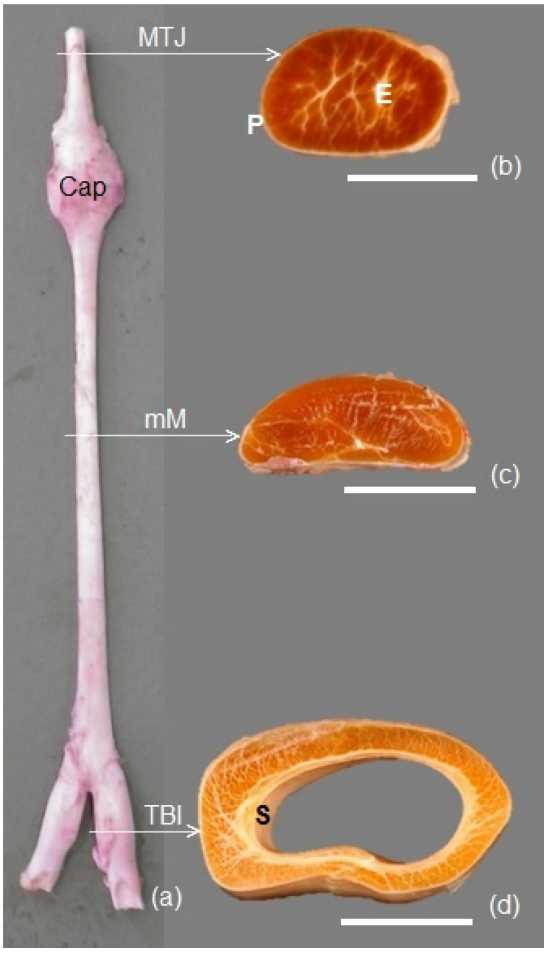

Fig. 1. Photograph of entire SDFT (a) and its cross-sectional images being oval at MTJ (b), semioval at mM (c), and ring-shaped at TBI (d). Outer surface of the whole tendon was enclosed by a thick peritendineum (P) which sent its endotendineum (E) into the tendon. Peritendineum and synovial sheath (S) was also found lining on the tunnel wall of TBI tendon. Bars=10 mm.

MATERIALS AND METHODS

Animals

The animals used in this experiment were approved by the Ethics Committee of Rakuno Gakuen University, Hokkaido, Japan. Superficial digital flexor tendons of the hindlimb were obtained from four clinically normal Holstein cows, aging 3.2, 3.5, 3.6 and 6.5 years old, which were used for another veterinary teachings without involvement with the locomotion system. The animals were tranquilized by giving an intramuscular injection of 0.2 mg/kg of xylazine (Bayer Yakuhin Co., Osaka, Japan), then anesthetized by giving an intramuscular injection of 20 mg/kg of pentobarbital sodium (Kyoritsu Seiyaku Co., Tokyo, Japan). Entire SDFT on the right hindlimb was immediately collected after the animals were euthanized by giving an intravenous injection of 0.2 mg/kg suxamethonium (Asuterasu Seiyaku Co., Tokyo, Japan).

Macroscopic observation

Appearance of the whole SDFTs was observed immediately after being dissected from the animals and the surrounding fat and paratenon was removed. Then, a piece of 5-mm-thick sample was perpendicularly sliced off at three different regions—immediately after emerging from gastrocnemius muscle or a few centimeters above the calcaneal cap (muscle-tendon junction, MTJ), the middle of metatarsus (mM), and the lateral part of this tendon inserting on the plantar surface of the middle phalanges of the fourth digit (tendon-bone interface, TBI) (Fig. 1a). After recording their cross-sectional shapes, their cross sectional areas (only solid areas) were analyzed by Image J (version 1.45s, National Institutes of Health, Bethesda, MD, U.S.A.).

Light and transmission electron microscopy

Three-cm-long samples being sectioned from each of the three designated regions (MTJ, mM, and TBI) were pre-fixed in a 3.0% glutaraldehyde fixative in 0.1 M phosphate buffer (pH 7.4) and tissue blocks of 1 × 1 × 3 cm were obtained from the center of each pre-fixed sample. Afterward, the tissue blocks were processed through the following steps; washed with 0.1 M phosphate buffer (pH7.4), post-fixed in 1.0% osmium tetroxide, washed with distilled water, dehydrated in graded ethanol series, and finally embedded in Quetol 812 (Nissin EM, Tokyo, Japan). Semithin (approximately 1.0 to 1.5 μm in thickness) and ultrathin sections (approximately 60 nm in thickness) were cut from the same areas with a Reichert Supernova system (Leica, Vienna, Austria) equipped with a diamond knife. The semithin sections were stained with toluidine blue, and observed and photographed by a light microscope. Number of tenocyte per 2.5 × 10^3 μm^2 was counted from eight photographs which were randomly selected from three tissue blocks of each individual by using Image J. The ultrathin sections were mounted on a copper grid and consecutively stained with 0.2% tannic acid in 10% ethanol in water for 15 min, 1.0% uranyl acetate for 5 min, and 1.0% lead citrate for 10 sec. A transmission electron microscope (TEM) (JEM-1220; JEOL, Tokyo, Japan) at an accelerating voltage of 80 kV was used for the

Table 1. Mean ± SD of the observed characteristics at the muscle-tendon junction (MTJ), middle metatarsus (mM) and tendon-bone interface (TBI)

Observed characteristics	MTJ	mM	TBI
Cross-sectional area (mm^2)*	129.9 ± 8.85[a)]	98.2 ± 11.97[b)]	144.7 ± 13.83[a)]
Cell count (cells/2.5 × 10^3 μm^2)**	5.2 ± 0.39[a)]	6.3 ± 0.26[b)]	10.0 ± 0.25[c)]
Collagen fibrils			
Diameter range (nm)	0–320	0–280	0–300
Diameter ≤100 nm (%)	34.2	49.3	67.0
Diameter ≥200 nm (%)	23.3	12.0	8.4
Minimum diameter	24.9 ± 11.73	22.5 ± 5.30	17.1 ± 5.52
1st quartile*	83.2 ± 22.10[a)]	65.9 ± 21.52[ab)]	43.3 ± 13.33[b)]
2nd quartile*	136.9 ± 24.95[a)]	103.8 ± 41.53[ab)]	69.5 ± 25.55[b)]
3rd quartile	193.6 ± 19.33	151.4 ± 55.96	132.5 ± 50.01
Maximum diameter	294.3 ± 24.45	224.5 ± 39.89	239.7 ± 54.71
CFI (%)*	81.8 ± 3.12[a)]	75.3 ± 1.70[b)]	73.1 ± 3.90[b)]
Water content (%)*	57.8 ± 2.98[a)]	63.1 ± 0.30[ab)]	65.9 ± 2.36[b)]
GAG chain			
Length (nm)*	19.5 ± 1.09[a)]	30.3 ± 3.69[ab)]	39.5 ± 6.29[b)]
Angle (°)**	49.9 ± 1.64[a)]	63.5 ± 1.75[b)]	75.3 ± 1.78[c)]

Different superscripted letters in each row indicate significant differences at $P<0.05$* or $P<0.0001$**.

investigation. Regards, diameters of 1,000 collagen fibrils were measured in ten photographs (100 fibrils per photograph) which were randomly selected from three tissue blocks per individual. Then, collagen fibril index (CFI) for characterizing the collagen-to-non-collagen ratio in ECM of per 2.5 × 10^5 nm^2 were analyzed by Image J.

Fresh tendon samples with a dimension of 1 mm^3 from the three regions were simultaneously fixed and stained with a solution containing 0.05% (w/v) cupromeronic blue, 0.1 M $MgCl_2$, 25 mM sodium acetate (pH 5.8), and 2.5% glutaraldehyde (w/v) for 5 days at 4°C. Further incubation with 0.034 M Na_2WO_4 was conducted at room temperature for 1 hr [19]. Ultrathin sectioning and TEM observation were conducted for the investigation of length and angle of sulfated GAG chains of decorin anchoring between two adjacent collagen fibrils. Three photographs which were randomly selected from three tissue blocks per individual were used for the measurement of length and angle of sulfated GAG chains by using Image J. Five GAG chains per photograph were measured.

Measurement of water content

The glutaraldehyde fixed samples, being collected from the medial TBI tendon, were cut into 2 × 2 × 2 mm blocks. Water content of each block was measured by heat drying type moisture meter (ML-50, A & D, Tokyo, Japan).

Statistical analysis

The numeric data were presented in mean ± standard deviation (mean ± SD). Only number of tendon cells were tested by non-parametric Steel Dwass method. The other morphometric aspects were tested by One-way ANOVA. Tukey multiple comparisons of means were applied to determine the differences between the three regions. All statistical significances were determined at $P<0.05$.

RESULTS

Morphology of the transected SDFT

After removal of the surrounding fat and paratenon connective tissue, cross-sectional shapes of the transected tendons were solid oval at MTJ, solid semioval at mM, and ring-shaped with a big hollow at TBI (Fig. 1b–d). Outer wall of the whole tendon and inner wall of the TBI tendon was wrapped by a thick trunk of peritendineum (epitenon) which sent its endotendineum (endotenon) or intratendinous trabeculae into the tendinous mass (Fig. 1b and 1d). Synovial sheath was also found to line over the innermost wall of the TBI tendon (Fig. 1d). The cross-sectional areas (mean ± SD, n=4) at MTJ, mM and TBI of SDFT were 129.9 ± 8.85, 98.2 ± 11.97 and 144.7 ± 13.83 mm^2, respectively (Table 1). Significant differences were seen only between the MTJ-mM and mM-TBI ($P<0.05$).

Population of tendon cell

The tendon cells were ubiquitously distributed in the tendon (Fig. 2). Nucleus of each cell occupied almost the whole perikaryon. Each cell sent out its cytoplasmic processes in all directions. Primary and secondary endotendineum was the intratendinous trabeculae of peritendineum being sent into the tendinous mass to form fascicles of different sizes. Each fascicle contained unequal number of tendon cells. Number of tendon cells per an area of 2.5 × 10^3 μm^2 was found increasing from 5.2 ± 0.39 at MTJ, 6.3 ± 0.26 at mM, to 10.0 ± 0.25 at TBI (Table 1). Significant differences among the three groups were observed at $P<0.0001$. In addition, water content in the tendons was varied from 57.8 ± 2.98% at MTJ, 63.1 ± 0.30% at mM and 65.9 ± 2.36% at TBI (Table

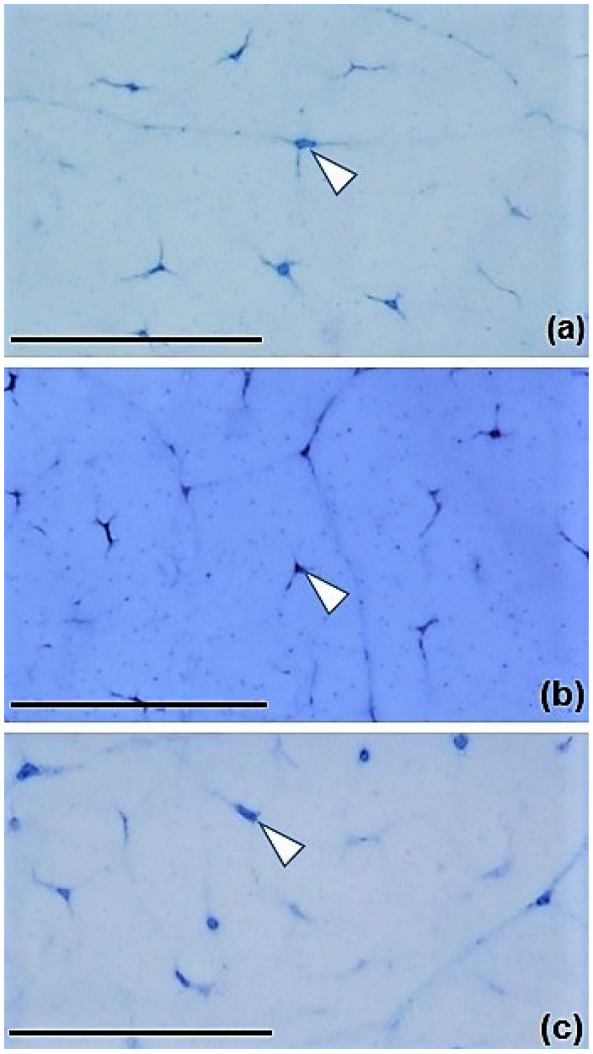

Fig. 2. Light microscopic images showing tendon cells (arrowheads) of SDFT at MTJ (a), mM (b) and TBI (c). Prominent nucleus at the cell bodies and certain number of cytoplasmic processes extended into the intercellular matrix were clearly observed. Bars=50 μm

1). Only the values between MTJ and TBI were found to be significantly different (P<0.05).

Morphometry of collagen fibrils

Collagen fibrils with different diameters and their distribution in the three transecting sites were clearly demonstrated in Fig. 3. Diameters of collagen fibrils were distributed within the range of 0–320 nm at MTJ, 0–280 nm at mM and 0–300 nm at TBI (Fig. 3, Table 1). Peak diameter of collagen fibrils at each site was within the range of 40–60 nm (Fig. 3). The percentage of thin collagen fibrils with diameters ≤100 nm was 34.2% at MTJ, but increased to 67% at TBI. However, the percentage of thick collagen fibrils with diameters ≥200 nm was 23.3% at MTJ, but decreased to 8.4% at TBI. The diameter data of each group were sorted from the smallest to the largest diameters, and then mean ± SD of minimum and maximum diameter, 1st–3rd quartiles, and maximum diameter values were presented in Table 1. Significances were seen only between MTJ and TBI in the 1st and 2nd quartile (P<0.05). Mean ± SD of CFI as an indicator of collagen fibril density in each diameter range was found decreasing from 81.8 ± 3.12% at MTJ, 75.3 ± 1.70% at mM, to 73.1 ± 3.90% at TBI (Table 1). Significant difference was found only between MTJ and TBI (P<0.05).

Length and angle of GAG chains

Cupromeronic blue staining could demonstrate the existence of GAG chains that connected between the neighboring fibrils (Fig. 4). Schematic diagram illustrating GAG chains was displayed in Fig. 5. Most GAG chains appeared in linear pattern with regular interval conforming the D-banding periodicity of the fibrillar microarchitecture. Length and angle of GAG chains stretching from one collagen fibril to the adjacent fibril was measured. Length of GAG chains increased from 19.5 ± 1.09 nm at MTJ, 30.3 ± 3.69 nm at mM, to 39.5 ± 6.29 nm at TBI (Table 1). Significant differences in GAG length was found only between MTB and TBI (P<0.05). Angles between GAG chains and collagen fibrils were also found to increase toward the distal portion, being 49.9°

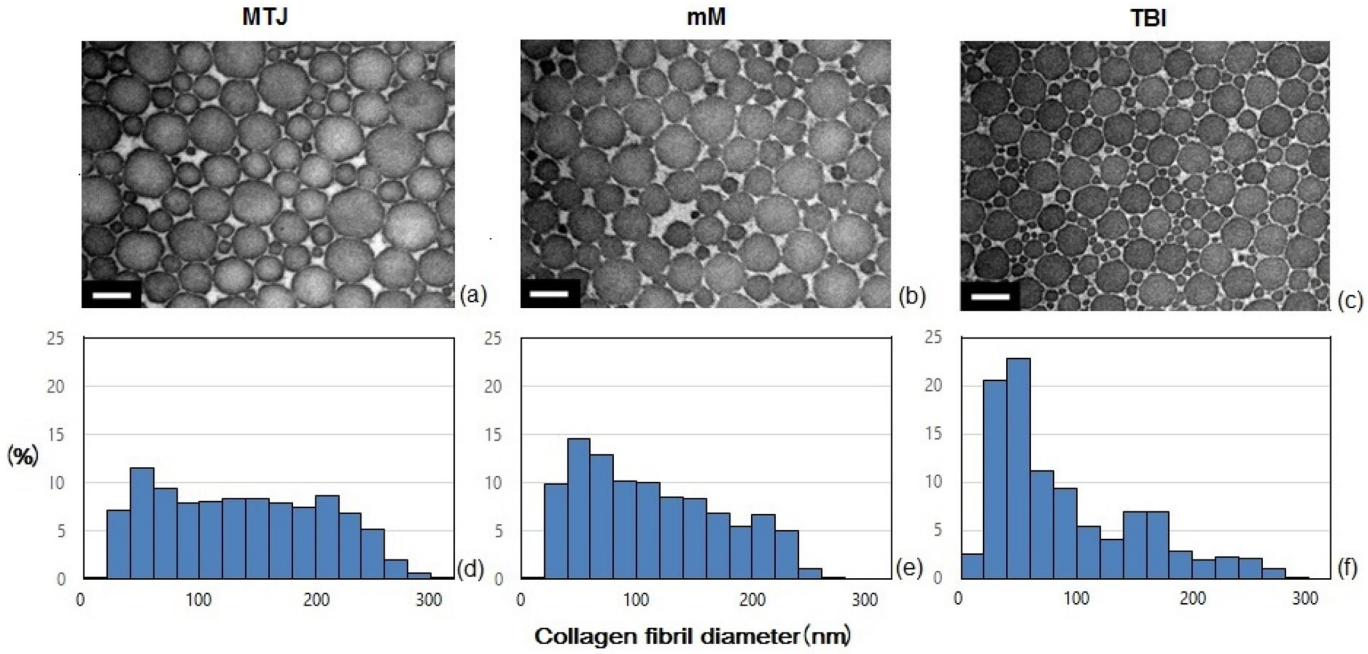

Fig. 3. Transmission electron microscopic images showing cross-sections of collagen fibrils and histograms showing diameter distribution of collagen fibrils of SDFT at MTJ (a, d), mM (b, e) and TBI (c, f). It was clearly seen that each area contained collagen fibrils of different diameters. Collagen fibrils with diameter ≥200 nm were abundant at MTJ, but that with diameter ≤100 nm was densely populated at TBI. Diameter distribution of collagen fibrils at mM was intermediate between its proximal and distal counterparts. Regards, mean ± SD of collagen fibril index (CFI) of MTJ, mM and TBI region was 81.8 ± 3.1, 75.3 ± 1.7 and 73.1 ± 3.9, respectively. Bars=200 nm.

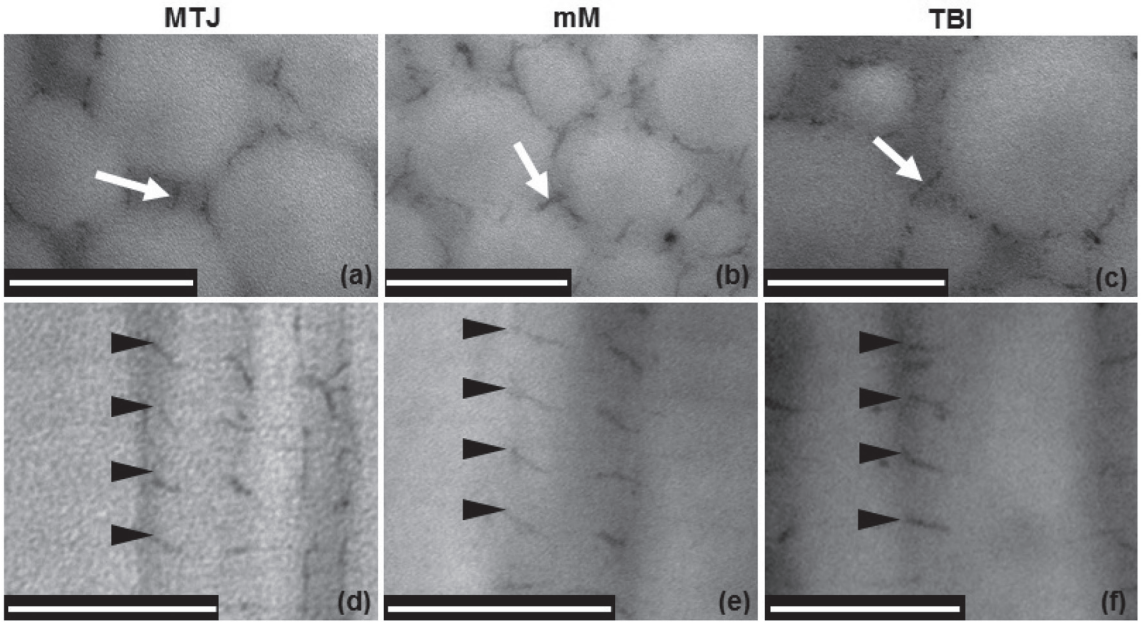

Fig. 4. Transmission electron microscopic images of SDFT with cupromeronic blue staining to demonstrate GAG chains stretching across the interfibrillar space. In the cross-sectional plane (a-c), mean ± SD of the length of GAG chains (arrows) being measured from one fibril to an adjacent fibril was 19.5 ± 1.1 at MTJ (a), 30.3 ± 3.7 at mM (b) and 39.5 ± 6.3 nm at TBI (c), respectively. In the longitudinal plane (d–f), mean ± SD of the angle of GAG chains (arrowheads) being measured against the longitudinal axis of collagen fibril was 49.9° ± 1.6 at MTJ (d), 63.5° ± 1.8 at mM (e) and 75.3° ± 1.8 at TBI (f), respectively. Bars=200 nm.

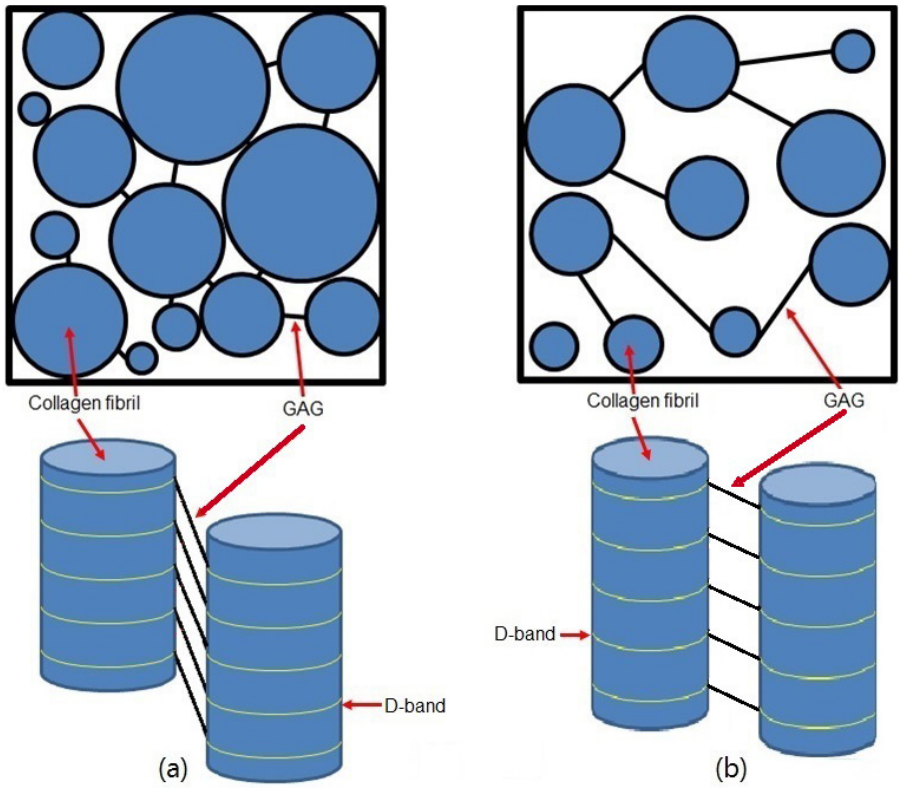

Fig. 5. Schematic drawing to demonstrate GAG chains interconnecting between collagen fibrils in SDFT with a higher (a) and lower CFI (b). Periodicity of GAG chains conforms the 67-nm-periodicity of D-banding pattern of the collagen fibrils. Tendon with higher CFI usually contains larger fibrils and narrower interfibrillar space, but that with lower CFI usually contains smaller fibrils and wider interfibrillar space. Collagen fibrils of tendon with higher CFI are likely to have longitudinal movement rather than lateral or horizontal movement as those having lower CFI. Regarding such movement, average angle of GAG chains of tendon with higher CFI is usually smaller than that with lower CFI.

± 1.64 at MTJ, 63.5° ± 1.75 at mM and 75.3° ± 1.78 at TBI (Table 1). Differences in GAG angles among the three groups were significant at $P<0.05$.

DISCUSSION

Variation in cross-sectional shapes of bovine SDFT, i.e. oval at MTJ, semioval at mM and ring-shaped at TBI, was similarly to that being observed at different regions along SDFT of equine forelimb [11, 26]. The differences in shape and diameter at each locality should have certain relationship with the attachment and adaptation to tension, compression, or friction from the adjacent structures [11, 16]. Regards, the oval shape of tendon at MTJ just emerging from the gastrocnemius muscle is a mere regular form of the tendon without receiving much compressive force from the adjacent structures. The flat surface of the semioval shape at the mM region is an adaptation to conform to the gliding surface of the deep digital flexor tendon (DDFT) coursing underneath. The hollow appearance in the vicinity of TBI with inner diameter about the size of the outer diameter of DDFT is its modification to provide a tunnel for the underneath DDFT to emerge to insert at the plantar surface of the distal phalanges [6]. Moreover, its thick synovial sheath covering inside the tunnel exists to reduce friction against the movement of the DDFT [8]. Table 1 showed that cross-sectional area of the tendon at MTJ and TBI was wider than that at mM. Since SDFT at MTJ is a gradual transformation from the superficial digital flexor (SDF) muscle, its diameter or surface area is still maintained as about the size the distal SDF muscle. After capping the calcaneal tuber, diameter of SDFT becomes smaller upon coursing behind the metatarsus, then turns larger at TBI. The increase in cross-sectional area of SDFT at TBI could provide a firm attachment between the tendon and bone; thus, allowing the efficient transmission of contractile force to the bone.

Functionally, mature collagen fibrils of different diameter can be classified into “thin” (diameter ≤100 nm) and “thick” (diameter ≥200 nm) fibrils [1, 14, 24]. Since collagen fibrils are the essential unit responsible for resisting tension of the tendon, distribution of fibril diameters is believed to associate with mechanical properties of tendon [5, 12]. The thick fibrils are aligned to withstand tension being exerted along with the long axis of the tendon. But the alignment of the thin fibrils is intended to withstand strains from different directions, such as flexion and horizontal compression [13, 14, 17]. Therefore, the differences in diameter range of collagen fibrils at any transected sites of the bovine tendon would reflect the axes of tension per se. Quantitative study in mouse tail tendon indicated that fibrils with small diameter dominate in young animal, but that with larger diameter dominate in older animal

[10]. However, SDFT, which is a weight-bearing and locomotory tendon being used in this study contains fibrillar population differently from that of the age-related non-weight-bearing tendon of mouse tail. Such observation also differed from the study in SDFT of the equine forelimb of different ages, either with or without physical training [12, 23, 26], especially at MTJ. The lower percentage of the thin fibrils but higher percentage of the thick fibrils at MTJ of the bovine tendon indicates a functional alignment in consistent with the properties of the SDF muscle which principally exerts in the longitudinal axis [26]. In contrast, a higher concentration of the thin fibrils but lower concentration of the thick fibrils at TBI should be a design of the bovine tendon to withstand the flexion and horizontal strains of the digits [17]. It is a matter of facts that the whole body weight exerts on both digits of each legs when the animal stands. Both digits are not only pushed toward their horizontal plane, but also pulled apart from each other. Degree of digital movement is dependent on the amount of weight exertion and strength of the tendon. Together with the digital movement, tendon at TBI that attached on each digit is also pulled and deviated from its original direction. Therefore, fibrils of the TBI tendon have to arrange in corresponding to such horizontal and abaxial or flexional movement of the digits. The distribution of collagen fibril diameters at the mM region is an intermediary between those of the MTJ and TBI. This transitional arrangement is expected to provide the tendon with an ability to resist tension from all directions. Besides the fibril diameter, other physical properties, such as length and width of fibrils and crosslink density, are also influential on the strength of collagen fibrils against breakage [24, 25].

CFI is the indicator of the density of collagen fibrils. Its value is inversely proportional to the distance of the interfibrillar space. Thus, a higher CFI at MTJ implies a higher density of collagen fibrils, but lower interstitial space and fluid content. Differently, the lower CFI at TBJ should infer a lower density of collagen fibrils, but higher interstitial space and fluid content [4]. Moisture in tendon is likely preserved by PG and GAG in the ECM. PG and their negatively charged GAG constituents are produced to attract large number of positive ions to increase the osmotic pressure [11]. This increased osmotic pressure helps retaining moisture in hydrated gel in ECM. This gel then imbues ECM with swelling pressure to resist compression [4]. It is apparent that tendon cells and fluid retention increase from MTJ towards TBI in response to the higher tensional and metabolic activities.

Collagen fibrils connect to each other by linear GAG chains which form ring mesh structure around each fibril [28]. The length of GAG chains in association with decorin that binds at D-band of the fibrils is highly relevant with the interfibrillar space [19–21, 27]. Thus, GAG chains of tendon with a higher CFI but narrower interfibrillar space should be shorter than that with a lower CFI but wider interfibrillar space. However, recruitment of GAG chains and decorin PGs into the stretched area may not be relevant to tensional resistance [7]. Each area of SDFT with hierarchical arrangement would response to tension differently, resulting in inconsistent longitudinal displacement of each fibril [3, 9, 13]. Distribution of diameter of collagen fibril is also a major factor dictating the directional response to tension. Collagen fibrils with large diameter are designed to have parallel orientation with greater resistance against high tensile strength. A reduction in diameter of collagen fibrils will increase surface area per unit mass of the fibrils to enhance the interfibrillar linkages between the fibrils and ECM [14, 15]. Distribution of collagen fibril diameter may be used for interpreting the mechanical properties of SDFT. Regards, the thick fibrils are prone to response to tension in the longitudinal direction while the thin fibril has tendency to response to bending and lateral deformation [13, 14, 17]. Such unequal longitudinal movement definitely yields a positive effect upon the angle of GAG chain—the longer the longitudinal displacement is, the smaller the angle will be; the shorter the longitudinal displacement is, the larger the angle will be. Since SDFT at MTJ contained the smallest amount of thin fibrils but the largest amount of the thick fibrils, this fibrillary component would respond to tension by having a certain degree of longitudinal rather than lateral movement. Such movement would yield the smallest average angle of GAG chain at MTJ upon comparing with its distal counterparts. On the other hand, the tendon at TBI contained the largest population of the thin fibrils but the smallest number of the thick fibrils. Such fibrillar composition should promote a lateral rather than longitudinal movement. Thus, the average GAG angle at TBI is the highest upon comparing with the other two areas. Fibrillar population at mM which is intermediate between its upper and lower sites should be relevant with the tension in transition between the two sites and compromise with the compressive force from the adjacent tendons. Moreover, the increase in water content would affect the function of tendon through disrupting its fibrillar components and interfering GAG contents [22].

In conclusion, different fibrillar arrangement at the three sites of SDFT of bovine hindlimb was a morphological adaptation to function in consistent with tensional axes and compressive force from the adjacent structures. Tendon at MTJ contains higher population of thick fibrils which align in response to longitudinal tension from the SDF muscle. In contrast, larger number of thin fibrils at TBI exists to withstand the flexion and horizontal strains. Fibrils at mM, having diameter intermediary between its proximal and distal counterparts, align to receive tension from all directions. Besides, strength of the tendon could be considered from the length, width and crosslink density of its fibrillar population.

REFERENCES

1. Adams, O. 2002 Disease and problems of tendons, ligaments, and tendon sheaths. pp. 594–598. *In*: Adams' Lameness in Horses, 5th ed. (Stashak, T. S. ed.), Lippincott Williams & Wilkins, Baltimore.
2. Anderson, D. E., St-Jean, G., Morin, D. E., Ducharme, N. G., Nelson, D. R. and Desrochers, A. 1996. Traumatic flexor tendon injuries in 27 cattle. *Vet. Surg.* **25**: 320–326. [Medline] [CrossRef]
3. Baer, E., Cassidy, J. J. and Hiltner, A. 1991. Hierachical structure of collagen composite systems: lessons from biology. *Pure Appl. Chem.* **63**: 961–973. [CrossRef]
4. Birk, D. E., Cohen, R., Geiger, B., Gumbiner, B., Hynes, R., Reichaedt, L., Ruoslahti, E., Trestad, R., Walsh, F. and Yurchenco, P. 1994. Cell junction, cell-cell adherens junction and extracellular matrix; Extracellular matrix of animals. pp. 971–995. *In*: Molecular Biology of the Cell, 3rd ed. (Alberts, B., Bray, D., Lewis, J., Raff, M., Roberts, K. and Watson, J. D. eds.), Garland Publishing, Inc., New York.

5. Dowling, B. A., Dart, A. J., Hodgson, D. R. and Smith, R. K. 2000. Superficial digital flexor tendonitis in the horse. *Equine Vet. J.* **32**: 369–378. [Medline] [CrossRef]
6. Dyce, K., Sack, W. and Wensing, C. J. G. 2009. The hindlimb of the ruminant. pp. 729–742. *In*: Textbook of Veterinary Anatomy, 4th ed., Saunders/Elsevier, St. Louis.
7. Fessel, G. and Snedeker, J. G. 2009. Evidence against proteoglycan mediated collagen fibril load transmission and dynamic viscoelasticity in tendon. *Matrix Biol.* **28**: 503–510. [Medline] [CrossRef]
8. Fisher, J. N., Di Giancamillo, A., Roveda, E., Montaruli, A. and Peretti, G. M. 2017. Functional morphology of muscles and tendons. *In*: Muscle and Tendon Injuries (Canata, G., d'Hooghe, P. and Hunt, K. eds.), Springer, Berlin.
9. Gautieri, A., Vesentini, S., Redaelli, A. and Buehler, M. J. 2011. Hierarchical structure and nanomechanics of collagen microfibrils from the atomistic scale up. *Nano Lett.* **11**: 757–766. [Medline] [CrossRef]
10. Goh, K. L., Holmes, D. F., Lu, Y., Purslow, P. P., Kadler, K. E., Bechet, D. and Wess, T. J. 2012. Bimodal collagen fibril diameter distributions direct age-related variations in tendon resilience and resistance to rupture. *J. Appl. Physiol.* **113**: 878–888. [Medline] [CrossRef]
11. Kannus, P. 2000. Structure of the tendon connective tissue. *Scand. J. Med. Sci. Sports* **10**: 312–320. [Medline] [CrossRef]
12. Magnusson, S. P., Hansen, P. and Kjaer, M. 2003. Tendon properties in relation to muscular activity and physical training. *Scand. J. Med. Sci. Sports* **13**: 211–223. [Medline] [CrossRef]
13. Ottani, V., Martini, D., Franchi, M., Ruggeri, A. and Raspanti, M. 2002. Hierarchical structures in fibrillar collagens. *Micron* **33**: 587–596. [Medline] [CrossRef]
14. Parry, D. A., Craig, A. S. and Barnes, G. R. 1978. Tendon and ligament from the horse: an ultrastructural study of collagen fibrils and elastic fibres as a function of age. *Proc. R. Soc. Lond. B Biol. Sci.* **203**: 293–303. [Medline] [CrossRef]
15. Parry, D. A. D., Barnes, G. R. G. and Craig, A. S. 1978. A comparison of the size distribution of collagen fibrils in connective tissues as a function of age and a possible relation between fibril size distribution and mechanical properties. *Proc. R. Soc. Lond. B Biol. Sci.* **203**: 305–321. [Medline] [CrossRef]
16. Puxkandl, R., Zizak, I., Paris, O., Keckes, J., Tesch, W., Bernstorff, S., Purslow, P. and Fratzl, P. 2002. Viscoelastic properties of collagen: synchrotron radiation investigations and structural model. *Philos. Trans. R. Soc. Lond. B Biol. Sci.* **357**: 191–197. [Medline] [CrossRef]
17. Raspanti, M., Ottani, V. and Ruggeri, A. 1990. Subfibrillar architecture and functional properties of collagen: a comparative study in rat tendons. *J. Anat.* **172**: 157–164. [Medline]
18. Russell, A. M., Rowlands, G. J., Shaw, S. R. and Weaver, A. D. 1982. Survey of lameness in British dairy cattle. *Vet. Rec.* **111**: 155–160. [Medline] [CrossRef]
19. Scott, J. E. 1992. Morphometry of cupromeronic blue-stained proteoglycan molecules in animal corneas, versus that of purified proteoglycans stained in vitro, implies that tertiary structures contribute to corneal ultrastructure. *J. Anat.* **180**: 155–164. [Medline]
20. Scott, J. E. 1993. Proteoglycans-fibrillar collagen interactions in tissue. pp. 165–181. *In*: Dermatan Sulfate Proteoglycan as a Tissue Organizer (Scott, J. E. ed.), Portland Press, London.
21. Scott, J. E. 1995. Extracellular matrix, supramolecular organisation and shape. *J. Anat.* **187**: 259–269. [Medline]
22. Sharma, P. and Maffulli, N. 2006. Biology of tendon injury: healing, modeling and remodeling. *J. Musculoskelet. Neuronal Interact.* **6**: 181–190. [Medline]
23. Smith, R. K., Birch, H., Patterson-Kane, J., Firth, E. C., Williams, L., Cherdchutham, W., van Weeren, W. R. and Goodship, A. E. 1999. Should equine athletes commence training during skeletal development?: changes in tendon matrix associated with development, ageing, function and exercise. *Equine Vet. J. Suppl.* **30**: 201–209. [Medline]
24. Tang, Y., Ballarini, R., Buehler, M. J. and Eppell, S. J. 2010. Deformation micromechanisms of collagen fibrils under uniaxial tension. *J. R. Soc. Interface* **7**: 839–850. [Medline] [CrossRef]
25. Wall, M. E. and Banes, A. J. 2005. Early responses to mechanical load in tendon: role for calcium signaling, gap junctions and intercellular communication. *J. Musculoskelet. Neuronal Interact.* **5**: 70–84. [Medline]
26. Watanabe, T., Imamura, Y., Hosaka, Y., Ueda, H. and Takehana, K. 2007. Graded arrangement of collagen fibrils in the equine superficial digital flexor tendon. *Connect. Tissue Res.* **48**: 332–337. [Medline] [CrossRef]
27. Watanabe, T., Hosaka, Y., Yamamoto, E., Ueda, H., Sugawara, K., Takahashi, H. and Takehana, K. 2005. Control of the collagen fibril diameter in the equine superficial digital flexor tendon in horses by decorin. *J. Vet. Med. Sci.* **67**: 855–860. [Medline] [CrossRef]
28. Watanabe, T., Kametani, K., Koyama, Y. I., Suzuki, D., Imamura, Y., Takehana, K. and Hiramatsu, K. 2016. Ring-mesh model of proteoglycan glycosaminoglycan chains in tendon based on three-dimensional reconstruction by focused ion beam scanning electron microscopy. *J. Biol. Chem.* **291**: 23704–23708. [Medline] [CrossRef]